Oscillations and negative velocity autocorrelation emerging from a Brownian particle model with hydrodynamic interactions

A. D. Viñales [1,*] M. Camuyrano [1,2] and G. H. Paissan [3,4]

[1]*Departamento de Física, Facultad de Ingeniería, Universidad de Buenos Aires, Avenida Paseo Colón 850, C1063ACV Buenos Aires, Argentina*

[2]*Comisión Nacional de Actividades Espaciales, Avenida Paseo Colón 751, C1063ACH Buenos Aires, Argentina*

[3]*CRUB, Universidad Nacional del Comahue, Quintral 1250, 8400 Bariloche, Río Negro, Argentina*

[4]*Centro Atómico Bariloche, CNEA/CONICET, Avenida Bustillo Km 9.5, 8400 Bariloche, Río Negro, Argentina*

(Received 15 August 2019; revised manuscript received 1 November 2019; accepted 6 May 2020; published 28 May 2020)

We study the dynamics of a particle in a fluid from a generalized Langevin equation (GLE) with a frictional exponential memory kernel and hydrodynamic interactions. By using Laplace analysis we obtain the analytical expressions for the velocity autocorrelation function (VACF) and mean square displacement (MSD) of the particle. Our results show that, in the strictly asymptotic time limit, the dynamics of the particle correspond to a particle ruled by a GLE with a Dirac delta friction memory kernel and hydrodynamic interactions. However, at intermediate times the dynamical behavior is qualitatively different due to the presence of a characteristic time in the frictional exponential memory kernel. Remarkably, the VACF exhibits oscillations and negative correlation regimes which are reminiscent of features already observed in pioneering works of molecular dynamics simulations. Moreover, ripples in the MSD appear as an emerging behavior associated with the mentioned regimes.

DOI: 10.1103/PhysRevE.101.052140

I. INTRODUCTION

In the first half of the twentieth century it was widely believed that the velocity autocorrelation function (VACF) had an exponential decay, as predicted by the stochastic theory. However, in the late 1960s the first computational simulations of molecular dynamics showed a slow characteristic decay, i.e., long-time tails of the VACF [1,2]. The numerical calculations, for a hard-core potential, established that the VACF has an asymptotic algebraic decay $\sim t^{-3/2}$ [3]. This algebraic decay was obtained from different theoretical approaches [4–9]. Experimental evidence supports this asymptotic behavior [10–15].

In addition to long-time tails, there are other dynamical features of the VACF observed in the early numerical experiments. Alder and Wrainwright [16] found negative temporal intervals of the VACF in molecular dynamics simulations for high densities of hard spheres [2,16]. Also Rahman showed negative correlations and an oscillatory behavior for the VACF in simulations of molecules of liquid argon interacting with a Lennard-Jones potential [1]. More recently, negative tails have been detected in supercooled liquid argon [17], supercooled liquid water [18], and hydrogen fluoride [19]. Oscillations have been observed in high-density amorphous ice [20]. Some features of the VACF such as oscillations and negative correlations have been studied from several theoretical approaches [21–23].

Also, the VACF and the mean square displacement (MSD) of a particle in a fluid have been studied in the theoretical frame of the generalized Langevin equation (GLE) with Basset and Stokes forces [24,25]. This framework has been applied in experimental research [26,27].

In particular, Mainardi and collaborators [28–30] modeled the movement of a particle in an incompressible viscous fluid. They used the classic viscous drag of the Stokes force, and incorporated the Basset force to take into account the retarding effects and the added mass. In the framework of a fractional Langevin equation they show that their model reproduces the asymptotic behavior of the VACF proportional to $t^{-3/2}$, and the linear temporal behavior of the MSD for long times corresponding to the normal diffusion. In addition, they found the analytical expression of the VACF as a combination of two Mittag-Leffler functions of order $1/2$. From this result they proved that the VACF is a monotonic decreasing function. Therefore they can obtain neither oscillations nor negative correlations of the VACF. Recently Grebenkov and Vahavi [24] considered a GLE in order to describe thermal motion of a tracer in a viscoelastic medium with Basset force and Stokes force. As frictional memory kernel of the Stokes force they used a power law $\sim t^{-\alpha}$ that recovers Mainardi's model for the particular case of a free particle with $\alpha = 1$, corresponding to normal diffusion.

An analytically solvable model of GLE with generalized Stokes force and hydrodynamic interactions that reproduces normal diffusion for long times, positive algebraic decay of the VACF $\sim t^{-3/2}$, oscillations, and negative correlations of the VACF is still missing in literature.

In this sense we propose a GLE model for a free Brownian particle with hydrodynamic interactions and frictional exponential memory kernel. We show that this model can

*avinales@fi.uba.ar

reproduce positive asymptotic decay of the VACF $\sim t^{-3/2}$ and the typical linear behavior of the MSD at sufficiently long times, i.e., normal diffusion. We obtain the analytical expressions of the VACF and MSD in terms of a finite sum of Mittag-Leffler functions, that allows us to do a complete theoretical analysis for all times. From a straightforward implementation we obtain oscillations and negative temporal intervals of the VACF and ripples in the MSD for certain values of the parameters involved.

This paper is organized as follows. In Sec. II we present a model for a free particle with a frictional memory kernel and hydrodynamic interactions. We also obtain the formal expressions of the VACF and the MSD since they are the magnitudes often reported in experimental papers; furthermore they characterize the dynamics of the particle. In Sec. III we obtain the analytical expressions of the VACF and MSD for the case of a free particle with an exponential frictional memory kernel and hydrodynamic interactions. Sec. IV is devoted to the analysis of the temporal behaviors of the VACF and the MSD. Finally, the conclusions are presented in Sec. V. In the Appendix we deal with some technical aspects related to the mathematical expressions of the VACF.

II. MODEL AND FORMAL EXPRESSIONS OF THE VACF AND THE MSD

Following Refs. [24,26,28–30] we consider a phenomenological model based on a GLE. The application of Newton's second law to a spherical particle of radius a and mass m produces

$$m\dot{v}(t) = F_S(t) + F_B(t) + F(t), \tag{1}$$

where $m = \frac{4}{3}\pi a^3 \rho_p$, with ρ_p the density of the particle. $F_B(t)$ is the Basset force that takes into account hydrodynamic interactions of a spherical particle of radius a with surrounding fluid [31]:

$$F_B(t) = -\frac{m_f}{2}\dot{v}(t) - 6a^2\sqrt{\pi\rho_f\eta}\int_{-\infty}^{t} dt' \frac{\dot{v}(t')}{(t-t')^{\frac{1}{2}}}, \tag{2}$$

where $m_f = \frac{4}{3}\pi a^3 \rho_f$, and ρ_f and η are the fluid density and viscosity respectively. The first term of Eq. (2) is related to the force due to the displaced mass of the fluid by the particle. The second term accounts for the retarded force due to the motion of the viscous unsteady flow around the sphere [32]. $F_S(t)$ is the generalized Stokes force with a friction memory kernel $\Gamma_s(t)$, which is usually used for modeling viscoelastic properties from the environment:

$$F_S(t) = -\int_{-\infty}^{t} dt' \Gamma_s(t-t') v(t'). \tag{3}$$

The random force $F(t)$ is a zero-centered and stationary Gaussian. Based on Refs. [28–30,33], Eq. (1) can be written as a generalized Langevin equation,

$$\dot{v}(t) + \int_{-\infty}^{t} dt' \gamma(t-t') v(t') = \frac{F(t)}{M}, \tag{4}$$

where

$$M = m + \frac{m_f}{2} = m\left(1 + \frac{r}{2}\right) \tag{5}$$

is the effective mass, and we have introduced the dimensionless parameter $r = \rho_f/\rho_p$. On the other hand, $\gamma(t)$ is the effective memory kernel,

$$\gamma(t) = \frac{\gamma_s}{\tau} e^{-t/\tau}\,\Theta(t) - \gamma_h \frac{t^{-3/2}}{2\sqrt{\pi}}\,\Theta(t), \tag{6}$$

where $\Theta(t)$ is the Heaviside step function.

The exponential term in the right side of Eq. (6) corresponds to the memory kernel in the Stokes force in our model, i.e., $\Gamma_s(t)/M = \frac{\gamma_s}{\tau} e^{-t/\tau}\,\Theta(t)$, where τ is the characteristic memory time of the friction interaction and γ_s is the friction coefficient for unit mass:

$$\gamma_s = \frac{6\pi a\eta}{M} = \frac{9}{(2+r)}\left(\frac{\eta}{\rho_p a^2}\right). \tag{7}$$

The parameter γ_h introduced in the second term of Eq. (6), given by

$$\gamma_h = \frac{6\pi a^2}{M}\sqrt{\rho_f \eta} = \frac{9\, r^{1/2}}{(2+r)}\sqrt{\frac{\eta}{\rho_p a^2}}, \tag{8}$$

characterizes the hydrodynamic interactions [24,26].

It is important to note from Eq. (8) that when $r \ll 1$, $\gamma_h \approx 0$, which corresponds to a heavy particle in comparison with the fluid (i.e., $\rho_p \gg \rho_f$). In this limit case the hydrodynamic interactions can be ignored and Eq. (1) corresponds to a GLE for a free particle without Basset force. On the other hand, the effects of the hydrodynamic interactions are more relevant when $r \gg 1$, which corresponds to a light particle in comparison with the fluid (i.e., $\rho_p \ll \rho_f$) [28].

Finally, we note that the random force $F(t)$ is connected with the effective memory kernel via the second fluctuation-dissipation theorem [34,35],

$$\langle F(t)F(t')\rangle = k_B T M\,\gamma(|t-t'|), \tag{9}$$

where k_B is the Boltzmann constant and T is the absolute temperature of the environment.

The calculations to follow are simplified by noting that Eq. (4) can be rewritten as [33,34,36]

$$\dot{v}(t) + \int_0^t dt' \gamma(t-t') v(t') = \frac{f(t)}{M}, \tag{10}$$

where the random force $f(t)$ in Eq. (10) is given by

$$f(t) = F(t) - M\int_{-\infty}^{0} dt' \gamma(t-t') v(t'). \tag{11}$$

From Eqs. (4), (9), (10), and (11) the random force $f(t)$ gets [33] the following properties:

$$\langle v(0) f(t)\rangle = 0, \tag{12}$$

$$\langle f(0) f(t)\rangle = k_B T M\,\gamma(|t|). \tag{13}$$

That is, the random force $f(t)$ does not correlate with $v(0)$ and obeys the second fluctuation dissipation theorem [34].

As is widely known, the velocity autocorrelation function contains fundamental dynamical information. In a normalized form, we write the VACF as

$$C_v(t) = \frac{\langle v(0)v(t)\rangle}{\langle v^2(0)\rangle}, \tag{14}$$

where $\langle v^2(0)\rangle = k_BT/M$. We multiply Eq. (10) by $v(0)$ to perform an ensemble average $\langle\,\rangle$, and by using Eqs. (12) and (14), we obtain

$$\dot{C}_v(t) + \int_0^t dt'\gamma(t-t')C_v(t') = 0. \tag{15}$$

Taking the Laplace transform of Eq. (15), we get

$$\widehat{C}_v(s) = \frac{1}{s+\widehat{\gamma}(s)}, \tag{16}$$

where $\widehat{\gamma}(s)$ is the Laplace transform of the effective memory kernel. The preceding equation is the first fluctuation dissipation theorem in the Laplace domain [28].

The MSD of a particle starting at the origin at $t_0 = 0$ is given by [28]

$$\langle x^2(t)\rangle = 2\,\langle v^2(0)\rangle \int_0^t dt_1 \int_0^{t_1} dt' C_v(t'). \tag{17}$$

From Eqs. (17) and (16) one can show that the Laplace transform of the MSD reads

$$\frac{\widehat{\langle x^2(s)\rangle}}{2\langle v^2(0)\rangle} = \frac{\widehat{C}_v(s)}{s^2} = \frac{s^{-2}}{s+\widehat{\gamma}(s)}. \tag{18}$$

Finally, note that Eq. (18) in the time domain reads

$$C_v(t) = \frac{1}{2\langle v^2(0)\rangle}\frac{d^2\langle x^2(t)\rangle}{dt^2}. \tag{19}$$

In the next section, we give explicit analytical expressions for the VACF and the MSD.

III. ANALYTICAL EXPRESSIONS OF THE VACF AND THE MSD

The Laplace transform of effective friction kernel given in Eq. (6) reads

$$\widehat{\gamma}(s) = \frac{\gamma_s}{1+s\tau} + \gamma_h s^{1/2}. \tag{20}$$

By inserting Eq. (20) in Eq. (16) we obtain the Laplace expression for $C_v(t)$, which reads

$$\widehat{C}_v(s) = \frac{1+s\tau}{\tau s^2 + \gamma_h\tau s^{3/2} + s + \gamma_h s^{1/2} + \gamma_s}. \tag{21}$$

It is worth noticing that, for $\tau = 0$, the Laplace inversion of Eq. (21) corresponds to the VACF obtained by Mainardi *et al.* [28], and for $\gamma_h = 0$ (without hydrodynamics interactions) it corresponds to the VACF of a free particle interacting with an exponential frictional memory kernel [37]. Equation (21) can be written as

$$\widehat{C}_v(s) = (1+s\tau)\widehat{G}(s), \tag{22}$$

where $G(t)$ is the Laplace inverse of

$$\widehat{G}(s) = \frac{1}{\tau s^2 + \gamma_h\tau s^{3/2} + s + \gamma_h s^{1/2} + \gamma_s}. \tag{23}$$

Therefore

$$C_v(t) = G(t) + \tau\, G'(t). \tag{24}$$

We rewrite Eq. (23) as

$$\frac{\tau}{\widehat{G}(s)} \equiv \tau^2 s^2 + \gamma_h\tau^2 s^{3/2} + s\tau + \gamma_h\tau s^{1/2} + \gamma_s\tau. \tag{25}$$

Following an approach similar to that given in Ref. [24], we introduce the variable $z = (s\tau)^{1/2}$, making Eq. (25) a polynomial in z of degree 4:

$$\frac{\tau}{\widehat{G}(s)} \equiv P(z) = z^4 + \gamma_h^* z^3 + z^2 + \gamma_h^* z + \gamma_s^*. \tag{26}$$

In this equation we have introduced the dimensionless parameters

$$\gamma_h^* = \gamma_h\tau^{1/2}, \tag{27}$$

$$\gamma_s^* = \gamma_s\tau \tag{28}$$

The polynomial $P(z)$ defined in Eq. (26) has four complex roots z_j, which can be obtained analytically by using the Ferrari formula [38]. Assuming that all roots are different (in the Appendix we show all possible cases), we write

$$\frac{1}{P(z)} = \prod_{j=1}^{4}\frac{1}{z-z_j} = \sum_{j=1}^{4}\frac{A_j}{z-z_j}, \tag{29}$$

where the coefficients A_j are

$$A_j = \frac{1}{[P'(z)]_{z=z_j}} = \prod_{k\neq j}^{4}\frac{1}{z_j - z_k}. \tag{30}$$

Now, we consider the following Laplace transform

$$\int_0^\infty dt\, e^{-st}\, t^{\beta-1}\, E_{\alpha,\beta}(ct^\alpha) = \frac{1}{s^{\beta-\alpha}(s^\alpha - c)}, \tag{31}$$

where $E_{\alpha,\beta}(y)$ is the generalized Mittag-Lefler function [39] defined by the series expansion

$$E_{\alpha,\beta}(y) = \sum_{j=0}^{\infty}\frac{y^j}{\Gamma(\alpha j+\beta)}, \quad \alpha > 0, \quad \beta > 0, \tag{32}$$

Introducing $z = (s\tau)^{1/2}$ in Eq. (29) and making use of Eq. (31), we obtain

$$G(t) = \sum_{j=1}^{4} A_j (t/\tau)^{-\frac{1}{2}} E_{\frac{1}{2},\frac{1}{2}}[z_j(t/\tau)^{\frac{1}{2}}]. \tag{33}$$

Using the identity

$$\frac{d}{dt}[E_\alpha(ct^\alpha)] = c\,t^{\alpha-1}\,E_{\alpha,\alpha}(ct^\alpha), \tag{34}$$

where $E_\alpha(y) = E_{\alpha,1}(y)$ is the one-parameter Mittag-Leffler function [40], we can write

$$G(t) = \sum_{j=1}^{4}\frac{A_j}{z_j}\tau\frac{d}{dt}[E_{\frac{1}{2}}[z_j(t/\tau)^{\frac{1}{2}}]]. \tag{35}$$

Taking into account the expression for the Mittag-Leffler derivative,

$$\frac{d}{dt}\left[E_{\frac{1}{2}}\left[z_j(t/\tau)^{\frac{1}{2}}\right]\right] = \frac{\tau^{-1/2}t^{-1/2}z_j}{\Gamma(1/2)} + \frac{{z_j}^2}{\tau}E_{\frac{1}{2}}[z_j(t/\tau)^{\frac{1}{2}}], \tag{36}$$

we get

$$G(t) = \sum_{j=1}^{4} A_j \frac{\tau^{1/2} t^{-1/2}}{\Gamma(1/2)} + \sum_{j=1}^{4} A_j\, z_j E_{\frac{1}{2}}\left[z_j (t/\tau)^{\frac{1}{2}}\right]. \quad (37)$$

Considering the sum rules for coefficients and roots of a polynomial [41],

$$\sum_{j=1}^{4} A_j (z_j)^m = 0, \quad m = 0, 1, 2, \quad (38)$$

and taking $m = 0$, we obtain

$$G(t) = \sum_{j=1}^{4} A_j\, z_j\, E_{\frac{1}{2}}[z_j (t/\tau)^{\frac{1}{2}}]. \quad (39)$$

Deriving Eq. (39), and using Eqs. (36) and (38), we arrive at

$$\tau\, G'(t) = \sum_{j=1}^{4} A_j\, {z_j}^3\, E_{\frac{1}{2}}\left[z_j (t/\tau)^{\frac{1}{2}}\right]. \quad (40)$$

Replacing Eqs. (39) and (40) in Eq. (24), we get the following expression of $C_v(t)$:

$$C_v(t) = \sum_{j=1}^{4} A_j\, (z_j + {z_j}^3) E_{\frac{1}{2}}[z_j (t/\tau)^{\frac{1}{2}}]. \quad (41)$$

In particular, applying the formula from [41]

$$\sum_{j=1}^{4} A_j (z_j)^3 = 1, \quad (42)$$

one can see that $C_v(0) = 1$, as we expected.

Using the identity [39]

$$\frac{\partial}{\partial t}\left[t^{\beta-1} E_{\alpha,\beta}(ct^{\alpha})\right] = t^{\beta-2} E_{\alpha,\beta-1}(ct^{\alpha}) \quad (43)$$

and Eq. (17), we can integrate the analytical expression of $C_v(t)$, given by Eq. (41), to obtain the analytical expression for $\langle x^2(t)\rangle$:

$$\frac{\langle x^2(t)\rangle}{2\tau^2\langle v^2(0)\rangle} = \sum_{j=1}^{4} A_j (z_j + {z_j}^3)(t/\tau)^2 E_{\frac{1}{2},3}\left[z_j (t/\tau)^{\frac{1}{2}}\right]. \quad (44)$$

The correlation functions given in Eqs. (41) and (44), which are expressed as a sum of four Mittag-Leffler functions of one and two parameters respectively, can be easily plotted. In the next section we make use of this fact to explore the temporal behavior of the correlation functions. In this sense it is important to introduce two dimensionless parameters. From Eqs. (27) and (28) we can obtain the following dimensionless parameter δ, related to the ratio of densities $r = \rho_f/\rho_p$:

$$\delta = \frac{\gamma_h^{*2}}{\gamma_s^*} = \frac{9\, r}{2 + r}, \quad (45)$$

where we used Eqs. (8) and (7). From Eq. (45) we can see that $0 < \delta < 9$; the limit cases correspond to $r = 0$ and $r = \infty$ respectively [28,29].

Also we can get another independent dimensionless scale number:

$$R = \frac{\delta}{\gamma_s^*} = \frac{a^2}{\nu\tau}, \quad (46)$$

where we have used Eqs. (7), (28), and (45). Also we have introduced the kinematic viscosity of the fluid given by $\nu = \eta/\rho_f$. Then Eq. (20) can be rewritten as

$$\widehat{\gamma}(s) = \widehat{\gamma}_1(s)(1 + \sqrt{R}\, z\, (1 + z^2)). \quad (47)$$

where $\widehat{\gamma}_1(s)$ is the first term of the right-hand side of Eq. (20), given by

$$\widehat{\gamma}_1(s) = \frac{\gamma_s}{1 + s\tau}. \quad (48)$$

From Eq. (47) we note that

$$\lim_{R\to 0} \widehat{\gamma}(s) = \widehat{\gamma}_1(s). \quad (49)$$

This limit case corresponds to a free particle interacting with an exponential frictional memory kernel.

Also after some algebra, Eq. (20) can be rewritten as

$$\widehat{\gamma}(s) = \widehat{\gamma}_2(s)\left(\frac{1 + \left(\frac{\sqrt{R}z}{1+\sqrt{R}z}\right)z^2}{1 + z^2}\right), \quad (50)$$

where $\widehat{\gamma}_2(s)$ is given by

$$\widehat{\gamma}_2(s) = \gamma_s + \gamma_h s^{1/2}, \quad (51)$$

which corresponds to Eq. (20) for $\tau = 0$, and is the Laplace transform of the effective memory kernel used by Mainardi *et al.* [28]. From Eq. (50) we see that

$$\lim_{R\to\infty} \widehat{\gamma}(s) = \widehat{\gamma}_2(s). \quad (52)$$

Therefore in this limit case the results presented in Ref. [28] are expected to be reobtained.

IV. TEMPORAL BEHAVIORS OF THE VACF AND THE MSD

The analytical expressions (41) and (44) are the main results of this work. In the following, we will analyze the time behaviors of the VACF and the MSD for different regimes. The short-time behaviors of these functions can be obtained by introducing the series expansion (32) in Eqs. (41) and (44). Then, in the short-time limit $t \to 0$ we get

$$\frac{\langle x^2(t)\rangle}{2\langle v^2(0)\rangle} \approx \frac{t^2}{2} - \frac{8\gamma_h}{15\sqrt{\pi}}\, t^{\frac{5}{2}}, \quad (53)$$

$$C_v(t) \approx 1 - \frac{2\gamma_h}{\sqrt{\pi}}\, t^{\frac{1}{2}} \quad (54)$$

where we have used Eqs. (38) and (42) and the result [41]

$$\sum_{j=1}^{4} A_j (z_j)^4 = -\gamma_h \tau^{1/2}. \quad (55)$$

The leading term of the expansion of MSD in Eq. (53) shows that the particle undergoes ballistic diffusion when the time is very small. The second term comes from the influence of the Basset force and it is independent of τ and γ_s. Therefore, the

expansion is the same as that obtained for the case where the friction memory kernel in the Stokes force is modeled by a white noise. The expression (53), to this order, is consistent with the analytical result from the VACF obtained by [24] with a friction memory kernel decaying as a power law (white noise corresponding to $\alpha = 1$). The expansion (54) for the VACF shows that it has a concave initial curvature due to the influence of the Basset force, and, as occurs with the MSD, the temporal behavior of the VACF is independent of τ and γ_s in the short-time limit.

Now, we obtain the temporal asymptotic behaviors of the VACF and the MSD at very long times, i.e., $t \to \infty$. Using Eqs. (18) and (21), and the thermic initial condition $\langle v^2(0)\rangle = \frac{k_B T}{M}$, we obtain

$$\frac{\widehat{\langle x^2(s)\rangle}}{2\frac{k_B T}{M}} = \frac{s^{-2}(s\tau + 1)}{\tau s^2 + \gamma_h \tau s^{3/2} + s + \gamma_h s^{1/2} + \gamma_s}. \tag{56}$$

For $s \to 0$ we get

$$\frac{\widehat{\langle x^2(s)\rangle}}{2\frac{k_B T}{M}} \approx \frac{s^{-2}}{\gamma_h s^{1/2} + \gamma_s} \approx \frac{s^{-2}}{\gamma_s}\left(1 - \frac{\gamma_h}{\gamma_s} s^{1/2}\right). \tag{57}$$

By Tauberian theorems [42] we derive the asymptotic expression of the mean square displacement for $t \to \infty$,

$$\langle x^2(t)\rangle \approx 2\frac{k_B T}{M}\frac{t}{\gamma_s} - 2\frac{k_B T}{M}\frac{\gamma_h}{{\gamma_s}^2}\frac{2\,t^{\frac{1}{2}}}{\sqrt{\pi}} \tag{58}$$

that can be written as

$$\langle x^2(t)\rangle \approx 2\,D\,t - 4\,D\,\frac{\gamma_h}{\gamma_s}\frac{t^{\frac{1}{2}}}{\sqrt{\pi}}, \tag{59}$$

where $D = \frac{k_B T}{M\gamma_s}$ is the diffusion coefficient. In the long-time limit, the MSD exhibits a linear behavior which corresponds to normal diffusion, i.e., $\langle x^2(t)\rangle \approx 2\,D\,t$. However, the Basset force, responsible for the algebraic decay of the velocity autocorrelation function, produces a retarding effect ($\propto t^{\frac{1}{2}}$) before the temporal linear behavior is established [28,30].

On the other hand, based on the relationship between the VACF and the MSD given in Eq. (19), we derived the asymptotic expression of $\langle x^2(t)\rangle$ given in Eq. (59) and we found that the asymptotic behavior of $C_v(t)$ for $t \to \infty$ is

$$C_v(t) \approx \frac{\gamma_h}{{\gamma_s}^2}\frac{t^{-\frac{3}{2}}}{2\sqrt{\pi}}. \tag{60}$$

As we point out in the Introduction, the long-time asymptotic behavior on the VACF ($\propto t^{-\frac{3}{2}}$) expressed by Eq. (60) was early observed by Alder and Wainwright in computer simulations [3] and it was also theoretically derived from different approaches. Our asymptotic expression for the VACF is in complete agreement with those equations obtained by Mainardi and collaborators [28,30]. However, as we will see, at intermediate times, from the main expressions Eqs. (41) and (44), the VACF and MSD respectively have significant qualitative and quantitative differences with those models.

The selection of ${\gamma_s}^*$ and ${\gamma_h}^*$ defines the dynamic characteristics of the system, since the ratio of densities between particle and fluid is set through δ [Eq. (45)] and also the scale number R [Eq. (46)] sets a relation between the kinematic viscosity, the size of the particle, and the Stokes memory characteristic time τ.

Taking into account the limit cases presented at the end of Sec. III, we have inspected the analytical expressions obtained for the VACF and MSD given by Eqs. (41) and (44) respectively, for different values of the parameters γ_h^* and γ_s^*.

In what follows, we present some results obtained from the calculation of the VACF and MSD given by Eqs. (41) and (44) respectively. In Fig.(1) we plot the VACF (41) as a function of t/τ for three sets of values of the dimensionless parameters γ_h^* and γ_s^*.

The upper panel Fig. 1(a) displays the VACF for $\gamma_h^* = 2$ and $\gamma_s^* = 1$; in this case, we obtain a positive monotonic decay for all times. In Fig. 1(b), corresponding to $\gamma_h^* = 0.5$ and $\gamma_s^* = 0.7472$, we can see that the VACF exhibits a different behavior with respect to the previous set of values shown in Fig. 1(a). The VACF remains positive as in Fig. 1(a) but it reaches a zero value. The inset in Fig. 1(b) is a magnification of the zone where the VACF takes its root, and shows that the curve remains positive without crossing the axes. A more complex dynamic behavior is obtained for $\gamma_h^* = 0.1$ and $\gamma_s^* = 5$, as we see in the lower panel Fig. 1(c). The VACF exhibits oscillations and multiple zero crossings, showing transitions between positive and negative correlations of the velocity. As we expected, the oscillations of the VACF attenuate and converge to zero with time. Note that the VACF has positive concavity at short times, according to Eq. (54). That is clearly seen in Fig. 1(a) and 1(b) but it would need a magnification at very short times in Fig. 1(c). Finally, in a schematic sense, the VACF in Fig. 1(b) can be understood as a limiting case between a strictly positive nonmonotonic decay and a nonmonotonic decay with zero crossings.

The MSD given by Eq. (44) is shown in Fig. 2 as a function of t/τ for the same set of parameters γ_h^* and γ_s^*, corresponding to the cases already shown for the VACF in Fig. 1. Figure 2(a) shows that the MSD of a particle, for $\gamma_h^* = 2$ and $\gamma_s^* = 1$, starts with a quadratic time dependency, in agreement with Eq. (53), which represents ballistic diffusion. Then, as expected, for sufficiently long times the MSD reaches a linear behavior which is typical of normal diffusion. We obtain a similar behavior for $\gamma_h^* = 0.5$ and $\gamma_s^* = 0.7472$ as we see in Fig. 2(b). But a different result occurs at intermediate times for $\gamma_h^* = 0.1$ and $\gamma_s^* = 5$, as shown in Fig. 2(c). A clear rippling appears at intermediate times in the MSD. These ripples correspond to the VACF presenting oscillations in Fig. 1(c), while Fig. 2(a) is associated with the VACF in Fig. 1(a) that has no oscillations. We know that the zero of the VACF in Fig. 1(b) does not have appreciable consequences on the MSD, as we see in Fig. 2(b).

Actually, the behaviors of MSD and VACF displayed in the results are related through Eq. (19). The concavity of the MSD is determined by the VACF sign; indeed the ripples observed in the plot of MSD are a consequence of sign changes on the VACF. The ripples observed in the plot of MSD, Fig. 2(c), are a consequence of sign changes of the VACF in Fig. 1(c). In addition, no ripple appears when the VACF has no change of sign, as shown in Figs. 1(a) and 1(b), where both cases have $C_v(t) \geqslant 0$ for all times.

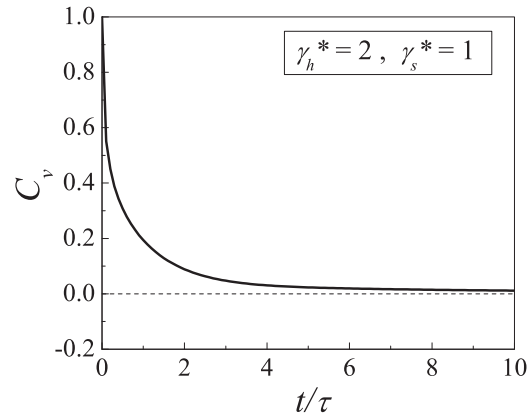

(a)

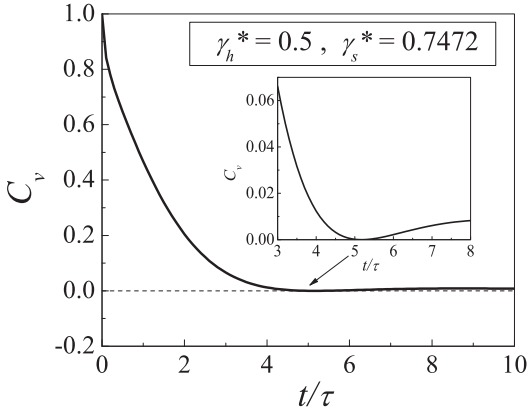

(b)

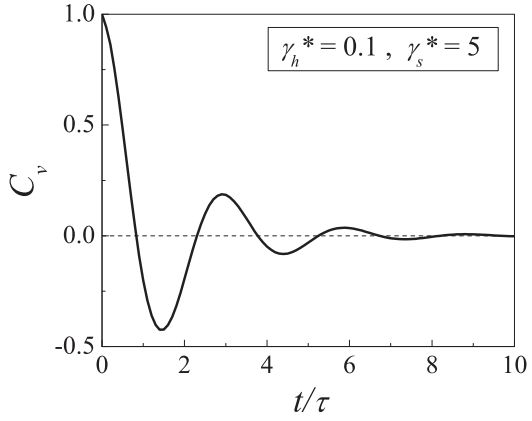

(c)

FIG. 1. Velocity autocorrelation function, $C_v(t)$, given by Eq. (41) as a function of t/τ, for different values of the dimensionless parameters γ_h^* and γ_s^*. Three types of behavior are exhibited: (a) monotonical decay for $\gamma_h^* = 2$ and $\gamma_s^* = 1$, (b) nonmonotonical decay limit with a zero but without zero crossings for $\gamma_h^* = 0.5$ and $\gamma_s^* = 0.7472$, (c) nonmonotonical decay with zero crossings for $\gamma_h^* = 0.1$ and $\gamma_s^* = 5$.

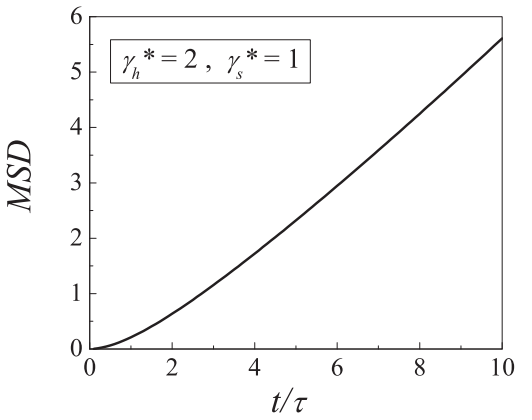

(a)

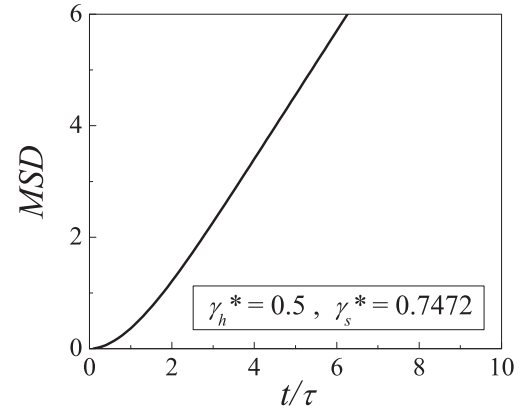

(b)

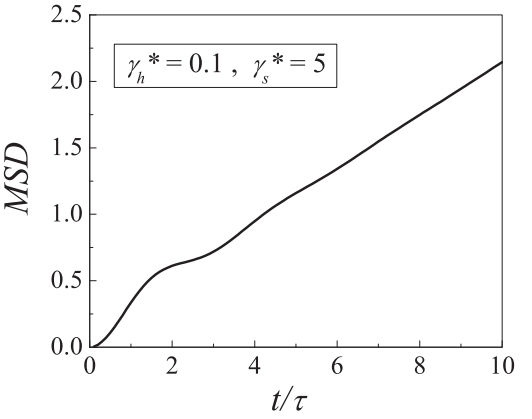

(c)

FIG. 2. Mean square displacement, MSD, given by Eq. (44) as a function of t/τ. For the same set of values presented in Fig. 1 we have (a) monotonical and concave up curve for $\gamma_h^* = 2$ and $\gamma_s^* = 1$, (b) monotonical and concave up curve for $\gamma_h^* = 0.5$ and $\gamma_s^* = 0.7472$, (c) monotonical behavior showing ripples at intermediate times for $\gamma_h^* = 0.1$ and $\gamma_s^* = 5$.

It is worth noting that the presence of ripples in the MSD have not been observed in the model presented by Mainardi *et al.* [30].

V. SUMMARY AND CONCLUSIONS

In this work we present a GLE model for a free particle interacting with the environment trough the Stokes and Basset forces. As the Stokes memory kernel we use an exponential function. We derive the analytical expressions for the VACF and the MSD. Our results, at short and long times, are consistent with those analytically obtained in previous models [24,30]. It is at intermediate times, in the transient state, where the model makes its main contribution. From the analytical expression of the VACF we obtain an oscillatory behavior and negative correlations for certain sets of parameters. These dynamical features resemble those that were observed from pioneering papers of molecular simulation.

On the other hand, the model presented by Mainardi and collaborators in [28], for a free particle interacting with a Stokes and Basset forces, uses a Dirac delta function as Stokes memory kernel [28–30]. They showed that the VACF is a decreasing function, completely monotonic and positive, tending to zero from above when $t \to \infty$. As a consequence, the corresponding expression for the VACF from that model provides neither negative correlations nor oscillations. Our results for the VACF show oscillations and negative correlations due to the fact that we introduce an exponential function as Stokes memory kernel in substitution of the Dirac's delta function. In this sense our model can be considered as an extension or generalization of their model. We explain the emerging features such as negative correlations and oscillations due to the introduction of a characteristic time through the exponential friction kernel. In this way, the present model catches characteristic physical aspects that have been observed on the VACF since the first simulations of molecular dynamics [1,2,16].

As we have shown in Eq. (49), the hydrodynamic interactions can be neglected when $R \to 0$, in this case the VACF corresponds to a free particle driven by an exponential noise. In this situation it is well known [37] that only three types of temporal behavior are obtained for the VACF: underdamped behavior for $\gamma_s^* > 1/4$, overdamped behavior for $\gamma_s^* < 1/4$, and critical behavior for $\gamma_s^* = 1/4$. From this analysis, we note that the oscillatory behavior obtained in Fig. 1(c) is in agreement with the expected result, since for this case $R = 0.0004 \ll 1$ and $\gamma_s^* = 5 > 1/4$, that corresponds to the underdamped behavior. One way to understand the physical meaning of the limit $R \to 0$ is to take the limit $\delta \to 0$ in Eq. (46). In accordance with Eq. (45), $\delta \to 0$ is a consequence of $r \to 0$, which corresponds to a heavy particle in comparison with the fluid (i.e., $\rho_p \gg \rho_f$).

On the other hand when $R \to \infty$ [Eq. (52)] we get the VACF obtained by Mainardi *et al.* [28]. Therefore for this limit case we expect a monotonic behavior for the VACF. Since $0 < \delta < 9$, the limit $R \to \infty$ only can be obtained when $\gamma_s^* \to 0$, and it can be achieved for $\tau \to 0$, which correspond to the model presented by Mainardi *et al.* [30]. They report a MSD without ripples [which is qualitatively similar to our result in Fig. 2(a)], and they show that it corresponds to an effective superdiffusion at intermediate times before reaching the normal diffusion regime. In contrast, our model does show ripples at intermediate times before the normal diffusion is established at long times, which suggests an alternation between effective superdiffusive and subdiffusive processes before reaching a regime of normal diffusion. Finally, let us note that the ripples in the MSD are a manifestation of the appearance of negative correlation of the velocity.

APPENDIX: ANALYSIS OF $P(z)$

From Eq. (26) we introduce

$$P_0(z) = P(z) - e = z^4 + bz^3 + z^2 + bz = z(z+b)(1+z^2), \tag{A1}$$

where $e = \gamma_s^*$ and $b = \gamma_h^*$, both positive numbers.

The roots of polynomial function $P_0(z)$ can be calculated immediately since it is easily factorized with two real roots $z_1 = 0$ and $z_2 = -b$ and two complex roots $z_3 = i$ and $z_4 = -i$.

It is easy to see that $P_0(z)$ and $P(z)$ share the minimum position $z_{\min}$ since the difference between them is only a constant; $z_{\min}$ is located between the real roots, that is, within the interval $(-b,\ 0)$, and can be obtained from

$$0 = \frac{dP_0(z)}{dz} = 4z^3 + 3bz^2 + 2z + b$$

We are interested only in the real root of this cubic polynomial, which is

$$z_{\min}(b) = -\frac{b}{4} + \frac{3\left[4\sqrt{b^4 - \frac{1}{3}b^2 + \frac{32}{27}} - b(b^2+4)\right]^{2/3} + 3b^2 - 8}{12\left[4\sqrt{b^4 - \frac{1}{3}b^2 + \frac{32}{27}} - b(b^2+4)\right]^{1/3}}. \tag{A2}$$

The type of roots of the polynomial function $P(z)$ are going to be determined by the minimum value of $P(z)$ given by $P(z_{\min}(b)) = P_0(z_{\min}(b)) + e$. Then there are three different situations:

(1) If $P(z_{\min}(b)) > 0$ or $e > -P_0(z_{\min}(b))$, there are no real roots, therefore there are two pairs of complex conjugate roots (four different complex roots)

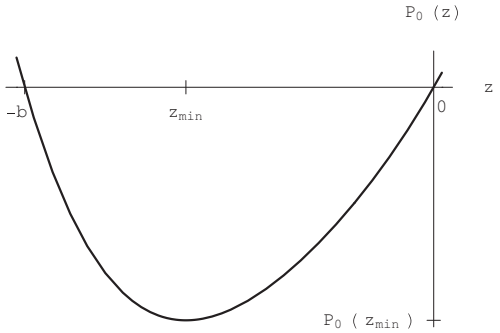

FIG. 3. Illustrative plot of $P_0(z) = P(z) - e$ that always presents two real roots: it has a root at zero and the other one at the negative number $-b$.

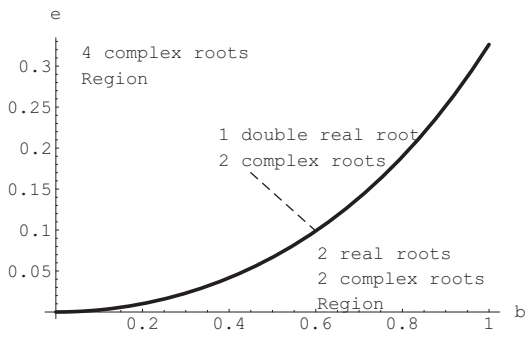

FIG. 4. Classification map in the e vs b parameter space for the type of roots of the polynomial function $P(z)$. The upper region corresponds to two complex roots and their complex conjugate. The lower region corresponds to two real roots, a complex root, and the corresponding complex conjugate. The solid line corresponds to a double real root, a complex root, and the corresponding complex conjugate one.

(2) If $P(z_{\min}(b)) = 0$ or $e = -P_0(z_{\min}(b))$, there are a double real negative root and two complex conjugate ones.

(3) If $P(z_{\min}(b)) < 0$ or $e < -P_0(z_{\min}(b))$, there are two different real negative roots and two complex conjugate roots.

Figure 4 shows two main regions for the set of parameters e and b. The upper region corresponds to $P(z)$ with four different roots (two different complex roots and the corresponding complex conjugate ones). The lower region corresponds to $P(z)$ with also four different roots (two different real roots, a complex root, and the complex conjugate one). The solid line that separates the two regions corresponds to $P(z)$ with a double real root, a complex root and the complex conjugate one.

Now we are going to prove that the polynomial function (26) cannot have two double complex roots. Since the polynomial function Eq. (26) has real and positive coefficients, if it has a complex root z_z then its conjugate $\bar{z}_z$ is also a root. Taking the conjugate of the polynomial function (26), we get

$$\bar{P}(z) = \bar{z}^4 + b\bar{z}^3 + \bar{z}^2 + b\bar{z} + e = P(\bar{z}). \tag{A3}$$

Then if z_z is a root of Eq. (26), $P(z_z) = 0$, using Eq. (A3) also $\bar{z}_z$ is a root of Eq. (26), $P(\bar{z}_z) = 0$. If it has two double complex roots z_1 and z_2, then they have to be complex conjugate, $z_2 = \bar{z}_1$. Then Eq. (26) can be written

$$P(z) = (z - z_1)^2(z - \bar{z}_1)^2, \tag{A4}$$

and it follows that

$$P(z) = z^4 - 4\,\mathrm{Re}\,(z_1)z^3 + 2(2[\mathrm{Re}\,(z_1)]^2 + |z_1|^2)z^2 - 4\,\mathrm{Re}\,(z_1)|z_1|^2 z + |z_1|^4. \tag{A5}$$

Comparing with Eq. (26) we obtain

$$b = -4\,\mathrm{Re}\,(z_1) = -4\,\mathrm{Re}\,(z_1)|z_1|^2, \tag{A6}$$

$$1 = 2\,(2[\mathrm{Re}\,(z_1)]^2 + |z_1|^2). \tag{A7}$$

From Eq. (A6) we obtain $|z_1| = 1$; replacing the result in Eq. (A7) we obtain

$$[\mathrm{Re}\,(z_1)]^2 = -\tfrac{1}{4}, \tag{A8}$$

which is an absurd result. Then Eq. (26) cannot have two double complex roots.

Finally it is straightforward to show that the polynomial cannot have a quadruple real root or two double complex roots.

[1] A. Rahman, Phys. Rev. **136**, A405 (1964).
[2] B. J. Alder and T. E. Wainwrigh, Phys. Rev. Lett. **18**, 988 (1967).
[3] B. J. Alder and T. E. Wainwrigh, Phys. Rev. A **1**, 18 (1970).
[4] R. Zwanzig and M. Bixon, Phys. Rev. A **2**, 2005 (1970).
[5] A. Widom, Phys. Rev. A **3**, 1394 (1971).
[6] K. M. Case, Phys. Fluids **14**, 2091 (1971).
[7] E. H. Hauge and M. Lof, J. Stat. Phys. **7**, 259 (1973).
[8] M. H. Ernst, J. Machta, J. R. Dorfman, and H. van Beijeren, J. Stat. Phys. **34**, 477 (1984).
[9] J. R. Dorfman, and E. G. D. Cohen, Phys. Rev. Lett. **25**, 1257 (1970).
[10] J. P. Boon and A. Bouiller, Phys. Lett. **55A**, 391 (1976).
[11] A. Bouiller, J. P. Boon, and P. Deguent, J. Phys. France **39**, 159 (1978).
[12] G. L. Paul and P. N. Pusey, J. Phys. A **14**, 3301 (1981).
[13] S. R. Williams, G. Bryant, I. K. Snook, and W. van Megen, Phys. Rev. Lett **96**, 087801 (2006).
[14] W. van Megen, J. Phys. Condens. Matter **14**, 7699 (2002).
[15] H. L. Peng, H. R. Schober, and T. Voigtmann, Phys. Rev. E **94**, 060601(R) (2016).
[16] B. J. Alder and T. E. Wainwrigh, in *Proceedings of the International Symposium on Transport Processes in Statistical Mechanics*, Brussels, August 27–31, 1956, edited by I. Prigogine (Interscience, London, 1958), pp. 97–131.
[17] A. De Santis, A. Ercoli, and D. Rocca, J. Chem. Phys. **119**, 9661 (2003).
[18] A. De Santis, A. Ercoli, and D. Rocca, J. Chem. Phys. **120**, 10194 (2004).
[19] E. Variyar, D. Kivelson, G. Tarjus, and J. Talbot, J. Chem. Phys. **96**, 593 (1991).
[20] J. S. Tse, D. D. Klug, C. A. Tulk, E. C. Svensson, I. Swainson, V. P. Shpakov, and V. R. Belosludov, Phys. Rev. Lett **85**, 3185 (2000).
[21] L. S. Reut and I. Z. Fisher, Ukr. Fiz. Zh. **12**, 1695 (1967).
[22] K. S. Singwi and M. P. Tosi, Phys. Rev. **157**, 153 (1967).
[23] T. V. Lokotosh, N. P. Malomuzh, and K. S. Shakum, J. Mol. Liq. **96-97**, 245 (2002).
[24] D. S. Grebenkov and M. Vahabi, Phys. Rev. E **89**, 012130 (2014).
[25] V. Lisý, J. Tóthová, and L. Glod, Int. J. Thermophys. **34**, 629 (2013).
[26] D. S. Grebenkov, M. Vahabi, E. Bertseva, L. Forró, and S. Jeney, Phys. Rev. E **88**, 040701(R) (2013).
[27] S. Buonocore, M. Sen, and F. Semperlotti, AIP Adv. **9**, 085323 (2019).

[28] F. Mainardi and P. Pironi, Extr. Math. **11**, 140 (1996).
[29] F. Mainardi and F. Tampieri, Technical Report No. 1, ISA0-TR-1/99, Istituto di Scienze dell'Atmosfera e dell'Oceano, CNR, Bologna, 1999 (unpublished).
[30] F. Mainardi, A. Mura, and F. Tampieri, Mod. Probl. Stat. Phys. **8**, 3 (2009).
[31] A. B. Basset, *A Treatise on Hydrodynamics, with Numerous Examples*, Vols. 1 and 2 (Deighton, Bell and Co., Cambridge, 1888).
[32] J. P. Boon and S. Yip, *Molecular Hydrodynamics* (Dover, New York, 1991).
[33] J. W. Dufty, Phys. Fluids **17**, 328 (1974).
[34] R. Kubo, M. Toda, and N. Hashitsume, *Statistical Physics II. Non-Equilibrium Statistical Mechanics* (Springer, Berlin, 1985).
[35] R. Zwanzig, *Nonequilibrium Statistical Mechanics* (Oxford University Press, New York, 2001).
[36] B. U. Felderhof, J. Phys. A: Math. Gen **11**, 921 (1978).
[37] A. D. Viñales and G. H. Paissan, Phys. Rev. E **90**, 062103 (2014).
[38] M. Abramowitz and L. Stegun, *Handbook of Mathematical Functions with Formulas, Graphs and Mathematical Tables* (Dover, New York, 1971).
[39] I. Podlubny, *Fractional Differential Equations* (Academic, London, 1999).
[40] F. Mainardi and R. Gorenflo, J. Comput. Appl. Math **118**, 283 (2000).
[41] K. S. Miller and B. Ross, *An Introduction to the Fractional Differential Equations* (Wiley, New York, 1993).
[42] G. Doetsch, *Introduction to the Theory and Apliccation of the Laplace Transformation* (Springer-Verlag, Berlin, 1974).